

Comparing high-speed video and Lightning Mapping Array observations to investigate the influence of ground strikes on lightning flash characteristics

Kate Ciampa, William Beasley, and Danyal Petersen

National Weather Center Research Experiences for Undergraduates Program, Norman, Oklahoma

This study presents exploratory observations for a set of 28 cloud-to-ground flashes recorded on high-speed video, each with a time resolution of 10,000 frames per second. The high time resolution, along with precise GPS timing, allows a detailed comparison of the videos with corresponding data from the Oklahoma Lightning Mapping Array (LMA). The LMA detects VHF radiation sources throughout the flashes, complementing the videos to provide a more complete visual understanding of flash development. We identify several interesting effects and phenomena related to the ground strike, and highlight the differences in flash development between cloud-to-ground flashes recorded on video and nearby intracloud flashes. Observations start with initial breakdown patterns in the flashes, contrasting initial structure of video cloud-to-ground flashes with that of the intracloud flashes. An initial descending discharge pattern is likely to terminate with a ground strike. The opposite initial pattern, a rising succession of source points, was observed in both some video recorded cloud-to-ground flashes and most nearby intracloud flashes. For cloud-to-ground flashes with an initial rise, abrupt changes in flash development can occur after the ground termination on video. In some cases, breakdown starts suddenly at new altitudes or locations, often associated with the beginning of new large-scale branches. The density of radiation source points can also change following a ground strike on video, often switching from dense, well-defined branching to sparser, more scattered discharge during the continuing current phase. Nearby intracloud flashes typically featured simultaneous defined and scattered breakdown, each developing in a separate layer.

1. Introduction

Early photographic studies investigated the optical properties of cloud-to-ground (CG) lightning with streak cameras, where movement of the film during exposure yielded a time-resolved image of stroke development (e.g. *Malan and Collens* 1937, *Kitagawa et al.* 1962). Careful analyses of streak photographs led to the first reports of the stepped leader stage (*Schonland et al.* 1935), and remarkably accurate estimates of the speed and duration of different flash stages (e.g. *Schonland et al.* 1938).

In the 1970s, researchers adapted television cameras for lightning video studies, gaining greater sensitivity and time resolution (*Winn et al.* 1973). However, standard video tape recordings contained a bias due to limited time resolution, as well as possible image persistence across frames (*Saba et al.* 2006a).

Development of digital high-speed video cameras circumvented these issues, offering a new level of detail with much higher time resolution. Several relatively recent studies present observations of natural lightning at frame rates ranging from one thousand to ten thousand frames per second, giving frame integration times of 1 millisecond to 100 microseconds. *Mazur et al.* (1995) used high-speed video at 1,000 fps, along with radio interferometer measurements, to study leaders, M events, and channel properties for a multiple-stroke CG flash. With video recordings at 1,000 to 8,000 fps, *Campos et al.* (2011) analyzed both positive and negative leader characteristics, combining their observations with electric field data to further study channel formation. In several Brazilian studies, high-speed imaging has

allowed researchers to determine parameters such as 2D leader speed, stroke multiplicity, and continuing current duration, statistical studies relying on accurate stroke counts (e.g. *Saba et al.* 2006b, *Ballarotti et al.* 2005). Similar studies employ high-speed video to verify the accuracy of CG lightning detection systems (*Ballarotti et al.* 2006).

While high-speed video cameras detect optical emissions during the CG stroke, lightning propagation also emits radiation at radio frequencies. These impulsive VHF radio emissions reveal the large-scale development of the flash throughout the thundercloud, and can be detected by VHF Lightning Mapping Arrays (LMA). The LMA system uses precise GPS time-of-arrival measurements from 6 or more stations to determine the source location geometrically for each pulse (*Hamlin* 2004, *Proctor* 1971). After detecting and locating many pulses, the LMA yields a 3-dimensional time sequence of points that correspond to discharge propagation.

This paper describes the combined use of high-speed digital videos and LMA data to examine cloud-to-ground lightning flashes and to investigate relationships between in-cloud (IC) discharges and ground flashes. Observations in this study highlight several interesting types of changes that can occur in the LMA discharge sequences in conjunction with the ground strikes captured with high-speed video. We focus on identifying possible effects the ground strike might have on the evolution of the discharge afterwards, as compared to what happens in similar nearby flashes that do not connect to ground.

2. Instrumentation and Methods

This study focuses on a data subset of 28 high-speed videos of CG lightning, recorded from May 2008 to May 2012 at the National Weather Center in Norman, Oklahoma. Each was recorded with a Photron SA1.1 high-speed digital video camera, at a time resolution of 10,000 frames per second. High luminosity frames, such as those at the beginnings of return strokes, set off the avalanche photodiode that automatically triggered video recording mode. Each Photron frame is GPS timestamped, accurate to within 10 μ s. The videos include time before and after the trigger frame, typically in a ratio of 1:3, with total times ranging from just over half a second to just

under a full second. Especially for flashes further away, the video timescale and field of view captured multiple strokes within flashes.

In digital viewing we could adjust various image parameters, most importantly the brightness, LUT, and zoom. Optimizing these factors added another level of visible detail to the structure of close up leaders, and enhanced the observations of M components and the continuing current stage. With brightness adjustments, we also saw low-luminosity return strokes and intracloud channel segments.

The region where the video-observed grounds strikes occurred is well within range of the Oklahoma LMA 3D capability. The LMA records the peak radiation event in each 80 μ s time interval, if it exceeds the noise threshold. When an event is detected at 6 or more stations, the LMA can determine its location in three special dimensions. The LMA also correlates the precise GPS timing with each pulse. In this study we use the time recorded in the high-speed video to identify a video CG flash from within a ten-minute segment of LMA data. Once the flash is isolated from others, we can focus in on specific features and animate the time sequence of radiation events, using the XLMA software developed at New Mexico Tech.

As an additional tool, we used data from the National Lightning Detection Network (NLDN) and Earth Networks total Lightning Network (ENTLN). For some cases, plotting the lightning detection network data along with LMA data aided in making a direct comparison of the timing in the videos with the sequence of development in the LMA plots. Lightning detection network data also helped identify nearby intracloud flashes.

3. Observations and case studies

3.1. Initial structure

The video-observed CG flashes in this study often exhibit well-defined initial breakdown patterns in LMA plots. We focused on the initial patterns in a video data subset of 28 CG flashes, each of which began within the range of 3D LMA capability. Twenty of the 28 CG flashes had relatively clear initial patterns in the LMA data. Fifteen of the 20 started with a downward succession of source points.

The initial descent seen on the time-altitude LMA plot is fairly thick, populated by a dense band of source points that dominate the discharge (as in Figure 1). Side view LMA plots reveal breakdown progression in one or more large-scale descending branches, one of which culminates in a ground strike on video. The time scale for this type of descent is on the order of tens of milliseconds, and the later part is often visible on video as the stepped leader stage.

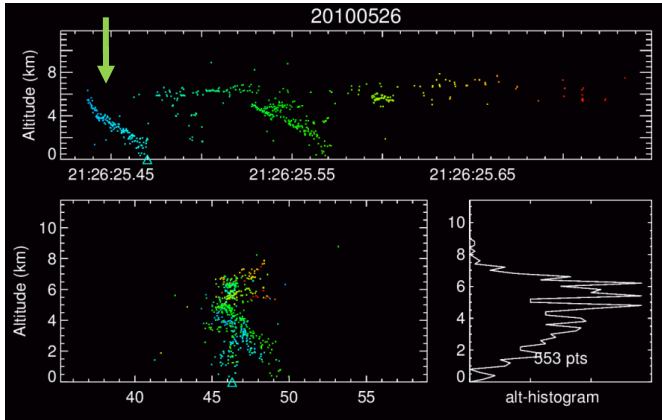


Figure 1. Time sequence and side view of initial descending breakdown.

In some cases, the LMA only detects a sparse descent of less than a dozen radiation sources, progressing quickly to ground. Figure 2a illustrates an example of a sparse descent for a 4/3/2012 video ground strike. Only about 7.5 ms pass between the first LMA point and the ground termination frame seen on video.

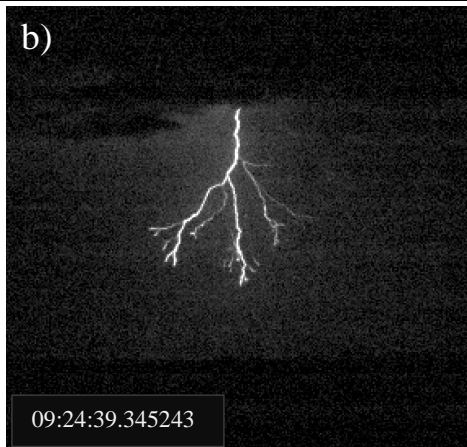
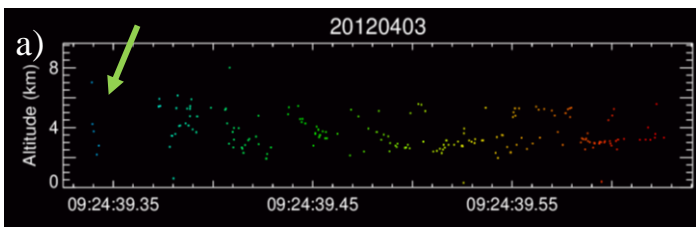


Figure 2. (a) Time sequence and (b) video frame of an initial sparse descent pattern.

Notice the highly branched structure of the leader in Figure 2b, indicating that a sparse LMA descent pattern does not imply a lack of branching.

While the initial descent is quite common, 5 video CG flashes actually began with an opposite pattern, in which discharge progresses upwards. Figure 3 shows the initial development in one of these flashes (the ground strike on video occurred in a later stage). After reaching the upper layer, breakdown decelerates and switches from vertical to horizontal propagation. A slight spread of the branch in the time-sequence plot corresponds to secondary branching seen in the top view and side view plots.

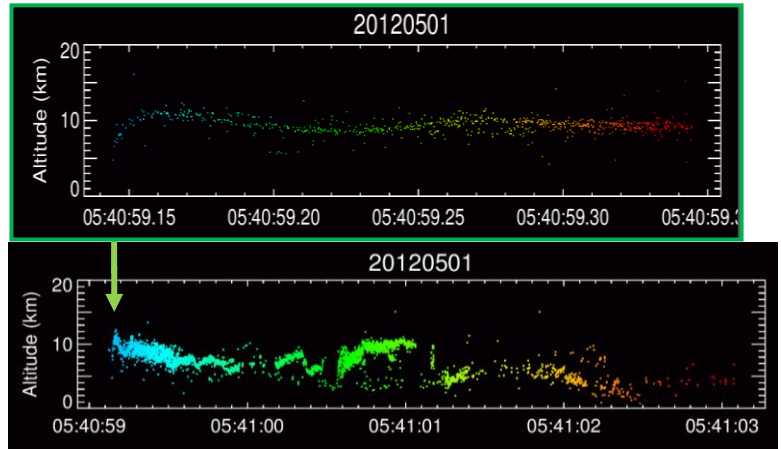


Figure 3. Time sequence of an initial rise pattern in a CG flash.

In nearby intracloud flashes, the initial rise was actually the predominant pattern, occurring in 31 of the 33 cases we studied. Each of these intracloud flashes occurred within 10 minutes of a video-observed ground strike, and in the region of 3D LMA capability. Figure 4 shows this phenomenon occurring in an IC flash, about two and a half minutes after several video ground strikes. The lower layer of discharge typically begins from the base of the upward rise, but is often delayed in the time sequence as *Shao and Krehbiel (1996)* observed.

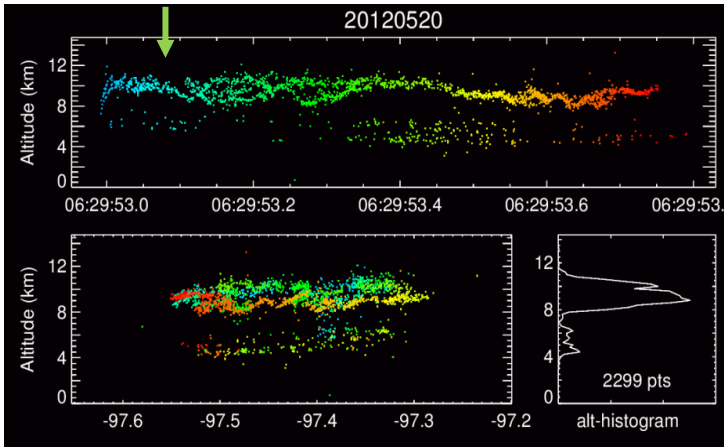


Figure 4. Time sequence and side view showing the initial rise pattern in an intracloud flash.

For both IC and CG flashes, the rapid upward breakdown pattern is not always limited to the beginning of flash development. It can also rise from the main layer of discharge later in the flash, sometimes many times, as further large-scale branches begin.

In addition, comparing time-altitude plots reveals a noticeable initial height difference between CG video flashes and nearby IC flashes. Among the flashes studied for initial patterns, the mean initial height on the LMA was 5.6 km for CG flashes, lower than the mean initial height of 7.8 km for the IC flashes.

3.2 Effects and phenomena following the ground strike

Directly after a ground strike on video, several types of changes can occur in flash development. These phenomena appear to be unique to CG flashes, and were not observed in nearby intracloud flashes. Figure 5 shows an interesting case where an abrupt change in discharge altitude immediately follows the ground strike on video. The descending branch ends with the ground strike, and then the tips of the other lower-level branches discharge during the return stroke. A new mid-level branch begins coincident with the continuing current phase on video, but its discharge is relatively scattered. This particular flash struck very close to the Weather Center, and the video shows the channel decay process in great detail. As the decay advances and the channel becomes fragmented, mid-level discharge lessens.

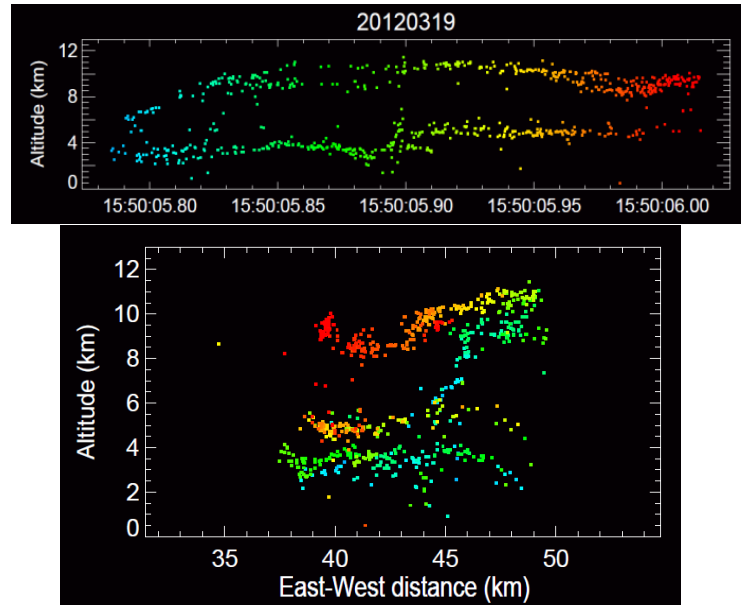


Figure 5. Time sequence and side view of a change in discharge altitude after a ground strike.

Some ground strikes on video are followed not only by a change in discharge height, but also a sudden change in location. In Figure 6, a portion of the 5/7/2008 video flash illustrates a particularly clear example of this feature. After a highly branched leader descent observed with both video and LMA, upper-level discharge begins within about 2 ms of the ground termination frame on video.

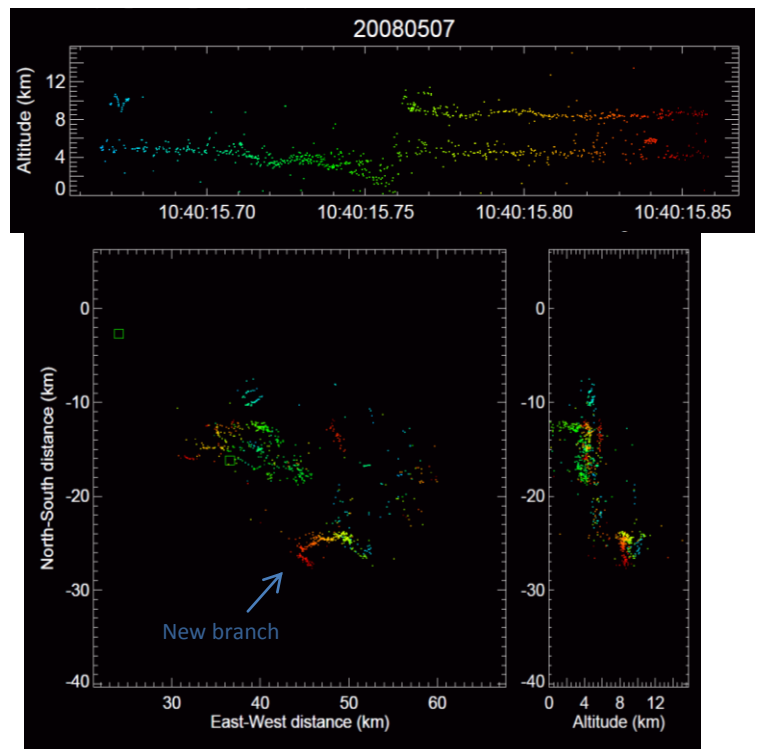


Figure 6. Time sequence and top view showing changes in discharge altitude and location after a ground strike.

The new branch begins about 15 kilometers to the southeast of the ground strike, requiring an average 2D propagation speed of at least 7.5×10^6 m/s to account for a causal connection between the ground strike and the new branch. Breakdown in this upper-level branch may act as a charge source for the current to ground, but not the only source, since the continuing current on video lasts more than 10 ms longer than the branch. However, the channel on video brightens slightly when discharge in the upper-level branch ceases, indicating the possibility of a lasting electrical connection.

In several cases, the high-speed videos capture a bit of intracloud activity along with the ground strike. When the timescales are on the order of tens of milliseconds, comparing these videos with corresponding time intervals in LMA data can be useful for investigating M components and continuing currents. Figure 7 shows an example of the M component process in a progression of video frames, each with 100 μ s time integration. The long horizontal branch appears to access charge stored in dark channels, allowing them a connection to ground and an illuminating current flow. The ground strike channel, receiving the additional current, brightens as well.

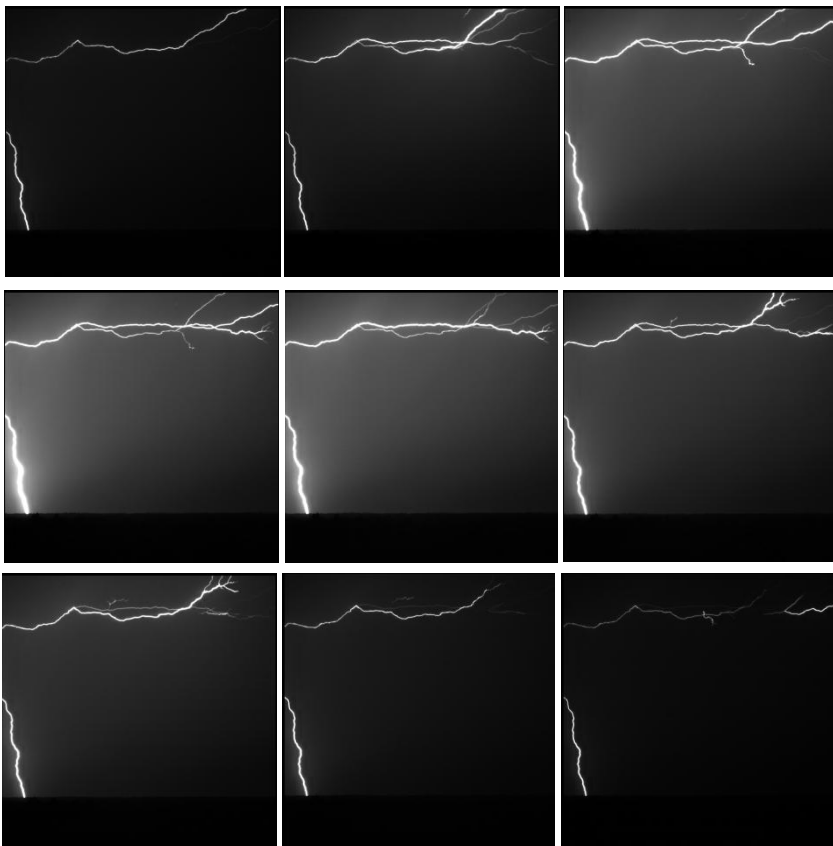


Figure 7. An M component event captured in a sequence of video frames at 10000 fps.

During the continuing current and M components of this stroke, VHF radiation spread in a scattered branching pattern with some small tight clumps of source points. The clumps mapped with the LMA may correspond to discharge in channel segments and recoil leaders, such as those seen in the video.

4. Concluding Remarks

A combination of observations of lightning at optical and VHF wavelengths yields a more complete picture of flash development than either data set alone. This study uses both high-speed videos and LMA data to investigate the structural characteristics of discharges in order to compare the in-cloud development of IC and CG flashes.

For many of the ground strikes on video, a downward breakdown sequence of VHF source locations dominates the initial flash structure, consistent with observations from *Shao and Krehbiel (1996)*. Subsequent return strokes and separate strokes on video are often also visible in the LMA data as distinct individual descent patterns. The second half of flash development stays primarily in the cloud, as discharges extend away from the region of the ground strike. However, the main channels appear to remain partially conductive, since discharges can propagate back rapidly and send down dart leaders even in the late stages of the flash. These are also seen on video when they occur close enough in space and time to the flash that triggered the video. For the cases where video CG flashes began with rising breakdown in VHF source locations, the first ground strike on video typically occurred in the later stages of the flash. Nearby intracloud flashes had discharge patterns similar to the beginning of the cloud-to-ground flashes, but they were generally shorter in duration and did not include the later, lower altitude stages in which discharges became more scattered.

In some cases, we observed changes in discharge altitude and location right after the ground strikes. These phenomena could possibly be consequences of the ground connection, since they were found in CG flashes recorded on video but not in nearby IC flashes. It also seems possible that they could be indirectly related as

consequences of preexisting fields or conductive channels. For flashes with early-stage video ground strokes, the subsequent changes in altitude were often less drastic. On the other hand, many of these cases did exhibit a significant decrease in radiation source density between and after ground strikes. In the side view LMA plots, this corresponded to slower scattered discharge growing from the tops of ground stroke channels.

Acknowledgements

We thank the National Science Foundation, Division of Atmospheric Sciences for support of this work under grant number NSF 0721119. We also thank Stan Heckman of Earth Networks for total lightning data, and Kristin Calhoun of the OU Cooperative Institute for Mesoscale Meteorology for lightning ground-strike data and assistance with LMA data. Many thanks also to Daphne LaDue and Amber Cannon for their direction of the Research Experiences for Undergraduates (REU) program at the National Weather Center.

References

Ballarotti, M. G., C. Medeiros, M. M. F. Saba, W. Schulz, and O. Pinto Jr. (2012), Frequency distributions of some parameters of negative downward lightning flashes based on accurate-stroke-count studies, *J. Geophys. Res.*, 117, D06112, doi:10.1029/2011JD017135.

Ballarotti, M. G., M. M. F. Saba, and O. Pinto Jr. (2005), High-speed camera observations of negative ground flashes on a millisecond-scale, *Geophys. Res. Lett.*, 32, L23802, doi:10.1029/2005GL023889.

Ballarotti, M. G., M. M. F. Saba, and O. Pinto Jr. (2006), A new performance evaluation of the Brazilian Lightning Location System (RINDAT) based on high-speed camera observations of natural negative ground flashes, paper presented at 19th International Lightning Detection Conference, Vaisala, Tucson, Arizona.

Campos, L. Z. S., M. M. F. Saba, O. Pinto Jr., and M. G. Ballarotti (2007), Waveshapes of continuing currents and properties of M-components in natural negative cloud-to-ground lightning from high-speed video observations, *Atmos. Res.*, 84, 302-310, doi:10.1016/j.atmosres.2006.09.002.

Campos, L. Z.S., M. M. F. Saba, W. Schulz, and O. Pinto Jr. (2011). Observations of natural cloud-to-ground lightning leaders from simultaneous high-speed video recordings and electric field measurements, 14th International Conference on Atmospheric Electricity, August 8-12, Rio de Janeiro, Brazil.

Ferro, M. A., M. M. F. Saba, and O. Pinto Jr. (2009) Continuing current in multiple channel cloud-to-ground

lightning, *Atmos. Res.*, 91, 399-403, doi:10.1016/j.atmosres.2008.04.011.

Fleenor, S. A., C. J. Biagi, K. L. Cummins, E. P. Krider, and X.-M. Shao (2009), Characteristics of cloud-to-ground lightning in warm-season thunderstorms in the Central Great Plains, *Atmos. Res.*, 91, 333-352, doi:10.1016/j.atmosres.2008.08.011.

Hamlin, T. D. (2004), The New Mexico Tech Lightning Mapping Array, Ph.D. dissertation, New Mexico Institute of Mining and Technology, Socorro.

Kitagawa, N., M. Brook, and E. J. Workman (1962), Continuing current in cloud-to-ground lightning discharges, *J. Geophys. Res.*, 67, 637– 647, doi:10.1029/JZ067i002p00637.

Kong, X. Z., X. S. Qie, Y. Zhao, and T. Zhang (2009), Characteristics of negative lightning flashes presenting multiple-ground terminations on a millisecond-scale, *Atmos. Res.*, 91, 381-386, doi:10.1016/j.atmosres.2008.03.025.

Lalande, P., A. Bondiou-Clergerie, G. Bacchiega, and I. Gallimberti (2002), Observations and modeling of lightning leaders, *C. R. Physique* 3, 1375-1392.

Lu, G., S. A. Cummer, J. Li, F. Han, R. J. Blakeslee, and H. J. Christian (2009), Charge transfer and in-cloud structure of large-charge-moment positive lightning strokes in a mesoscale convective system, *Geophys. Res. Lett.*, 36, L15805, doi:10.1029/2009GL038880.

Lu, G., S. A. Cummer, R. J. Blakeslee, S. Weiss, and W. H. Beasley (2012), Lightning morphology and impulse charge moment change of high peak current negative strokes, *J. Geophys. Res.*, 117, D04212, doi:10.1029/2011JD016890.

Malan, D. J., and H. Collens (1937), Progressive lightning, III, The fine structure of return lightning strokes, *Proc. R. Soc. London, Ser. A*, 162, 175– 203.

Mazur, V. (2002), Physical processes during development of lightning flashes, *C. R. Physique* 3, 1393-1409.

Mazur, V., P. R. Krehbiel, and X.-M. Shao (1995), Correlated high-speed video and radio interferometric observations of a cloud-to-ground lightning flash, *J. Geophys. Res.*, 100, 25,731-25,753.

Pawar, S. D., and A. K. Kamra (2004), Evolution of lightning and the possible initiation/triggering of lightning discharges by the lower positive charge center in an isolated thundercloud in the tropics, *J. Geophys. Res.*, 109, D02205, doi:10.1029/2003JD003735.

Proctor, D. E. (1971), A hyperbolic system for obtaining VHF radio pictures of lightning, *J. Geophys. Res.*, 76, 1478– 1489.

Qie, X., et al. (2005) The possible charge structure of thunderstorm and lightning discharges in northeastern verge of Qinghai–Tibetan Plateau, *Atmos. Res.*, 76, 231-246, doi:10.1016/j.atmosres.2004.11.034.

- Saba, M. M. F., M. G. Ballarotti, and O. Pinto Jr. (2006a), Negative cloud-to-ground lightning properties from high-speed video observations, *J. Geophys. Res.*, 111, D03101, doi:10.1029/2005JD006415.
- Saba, M. M. F., O. Pinto Jr., and M. G. Ballarotti (2006b), Relation between lightning return stroke peak current and following continuing current, *Geophys. Res. Lett.*, 33, L23807, doi:10.1029/2006GL027455.
- Saba, M. M. F., K. L. Cummins, T. A. Warner, E. P. Krider, L. Z. S. Campos, M. G. Ballarotti, O. Pinto Jr., and S. A. Fleenor (2008), Positive leader characteristics from high-speed video observations, *Geophys. Res. Lett.*, 35, L07802, doi:10.1029/2007GL033000.
- Schonland, B. F. J., D. J. Malan, and H. Collens (1935), Progressive lightning II, *Proc. R. Soc. London, Ser. A*, 152, 595–625.
- Schonland, B. F. J., D. J. Malan, and H. Collens (1938), Progressive lightning IV, *Proc. R. Soc. London, Ser. A*, 168, 455–469.
- Shao, X. M., and P. R. Krehbiel (1996), The spatial and temporal development of intracloud lightning, *J. Geophys. Res.*, 101, D21, doi:10.1029/96JD01803.
- Wiens, K. C., S. A. Rutledge, and S. A. Tessendorf (2005), The 29 June 2000 supercell observed during STEPS. Part II: Lightning and charge structure, *J. Atmos. Sci.*, 62, 4151–4177.
- Winn, W. P., T. V. Aldridge, and C. B. Moore (1973), Video Tape Recordings of Lightning Flashes, *J. Geophys. Res.*, 78(21), 4515–4519, doi:10.1029/JC078i021p04515.